

# Some advances in high-performance finite element methods

Finite element  
methods

Song Cen, Cheng Jin Wu and Zhi Li

*School of Aerospace Engineering, Tsinghua University, Beijing, China*

Yan Shang

*College of Aerospace Engineering,  
Nanjing University of Aeronautics and Astronautics, Nanjing, China, and*

Chenfeng Li

*College of Engineering, Swansea University, Swansea, UK*

2811

Received 28 October 2018  
Revised 28 December 2018  
Accepted 11 January 2019

## Abstract

**Purpose** – The purpose of this paper is to give a review on the newest developments of high-performance finite element methods (FEMs), and exhibit the recent contributions achieved by the authors' group, especially showing some breakthroughs against inherent difficulties existing in the traditional FEM for a long time.

**Design/methodology/approach** – Three kinds of new FEMs are emphasized and introduced, including the hybrid stress-function element method, the hybrid displacement-function element method for Mindlin–Reissner plate and the improved unsymmetric FEM. The distinguished feature of these three methods is that they all apply the fundamental analytical solutions of elasticity expressed in different coordinates as their trial functions.

**Findings** – The new FEMs show advantages from both analytical and numerical approaches. All the models exhibit outstanding capacity for resisting various severe mesh distortions, and even perform well when other models cannot work. Some difficulties in the history of FEM are also broken through, such as the limitations defined by MacNeal's theorem and the edge-effect problems of Mindlin–Reissner plate.

**Originality/value** – These contributions possess high value for solving the difficulties in engineering computations, and promote the progress of FEM.

**Keywords** Hybrid displacement-function (HDF), Hybrid stress-function (HSF), Mesh distortion, Fundamental analytical solutions, High-performance finite element methods, Improved unsymmetric finite element method

**Paper type** General review

## 1. Introduction

As the cornerstone of computational mechanics, the finite element method (FEM) is recognized as one of the greatest achievements in the twentieth century (Feng and Shi, 2006; Bathe, 1996; Long *et al.*, 2009; Turner *et al.*, 1956; Zienkiewicz and Taylor, 2000). During the past 70 years, with the progress of computer technology, the FEM also obtained great developments in its theories and applications, and has become the main computation and simulation tool in science and engineering. It is undeniable that, a quite completed system of



The authors would like to thank the National Natural Science Foundation of China (11872229, 11702133), the Natural Science Foundation of Jiangsu Province (BK20170772) and the Project Funded by the Priority Academic Program Development of Jiangsu Higher Education Institutions.

the FEM has been formed, and can be applied for computing and simulating almost all problems with macro scale in continuum mechanics (Long and Cen, 2001; Lu *et al.*, 2015; Lu *et al.*, 2018; Zhang and Cen, 2016). However, any user of the FEM must realize that, the traditional FEM is only a pure numerical method that depends on patch interpolation techniques. Therefore, from the viewpoints of the mathematics and computer technology, some inherent defects are inevitable. In some special occasions, uncorrected results may easily appear if some little details are overlooked.

It is well known that in a finite element analysis, the computation must be performed by using a mesh composed of various finite elements. In other words, the mesh is an essential part of the FEM, in which each element is the domain for interpolation, integration and computation in element level. Unfortunately, some troubles are just caused by the mesh. To ensure computation precision, those meshes composed of elements with only regular shapes are strongly anticipated. Once a distorted mesh is used, the accuracy may drop dramatically (Lee and Bathe, 1993). Various numerical problems, such as shear locking, volume locking, and so on, will appear. Figure 1a shows a rectangular beam under pure bending condition (plane stress state). The exact solutions for displacements and stresses can be obtained if only one rectangular eight-node isoparametric element Q8 with full integration is used (Figure 1b). However, if five distorted Q8 elements with full integration are used (Figure 1c), the relative errors will exceed 90 per cent. This is the sensitivity problem to mesh distortion, an inherent difficulty existing in the FEM for a long time. For warning users to avoid unreliable results, many commercial CAE software products, such as Simula/Abaqus, will check the mesh and report the proportion of the distorted elements (Abaqus, 2009).

At present, few effective ways for eliminating the influence caused by distorted mesh can be found. All people must pay attention to the mesh quality. Nevertheless, for those solids and structures with complex configurations, it is not easy to achieve the goal. In the 3D problem, the hexahedral elements usually possess much better precision and efficiency than the tetrahedral ones. Up to date, the automatic 3D mesh generation technique of hexahedral elements is still a challenging problem in finite element modeling (Cheng and Zhang, 2007). That is to say, the mesh distortion problem is almost inevitable in the mesh composed of hexahedral elements for the 3D solids with complex shapes. Some researchers suggested to resist mesh distortion problem with reduced integration in elements. However, the hourglass (over soft) problems may take place in local region where the reduced integration elements exist, and the precision for stress solutions cannot be guaranteed (Zhuang *et al.*, 2005). The

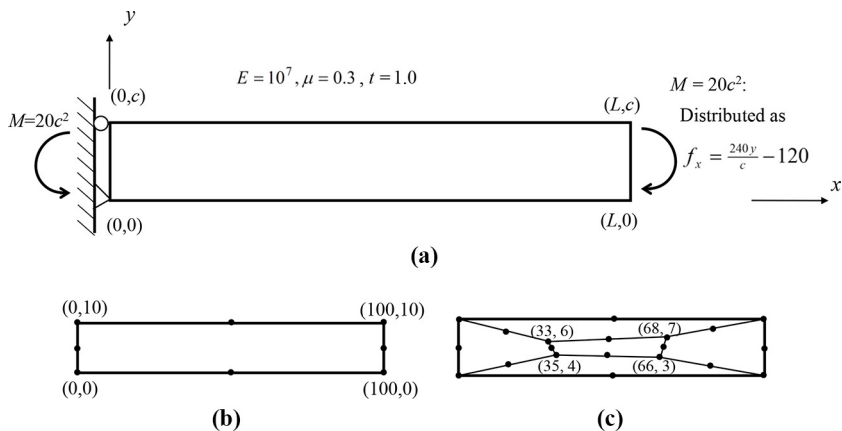
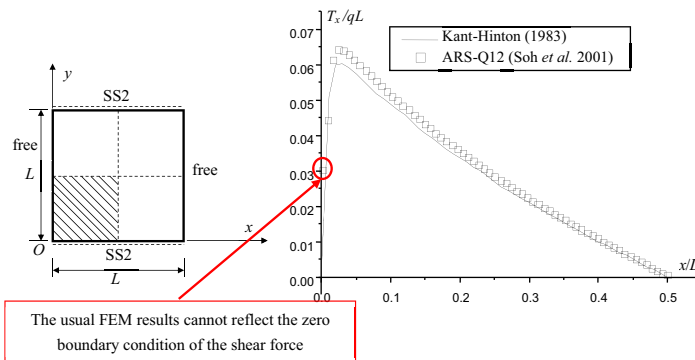


**Figure 1.**  
Pure bending beam  
calculated by plane  
eight-node elements  
(Lee and Bathe, 1993)

refined mesh is another treatment for overcoming mesh distortion. But if the number of elements is huge, the computation cost for highly nonlinear or dynamic problems will increase at an  $N^3$  rate. Furthermore, it seems that mesh distortions always occur for large deformation state.

In crack propagation problems, some other troubles will be also caused by the finite element mesh. For example, when simulating crack propagation, different meshes may lead to different propagation directions. And remeshing the structures after crack propagation is a big problem because a great deal of distorted elements will appear along the winding propagation path. To break above obstacles, Belytschko *et al.* (1994) proposed an element-free Galerkin method. From that time, various element-free, mesh-free, and meshless methods have been appearing in numerous literatures. By combination of the techniques from CAD, FEM and NURBS (Non-Uniform Rational B-Splines), Hughes *et al.* (2005) proposed an exact geometry method for numerical modeling. This method, denoted by isogeometric analysis, has become a research hotspot in recent years. For avoiding mesh dependence problem and remeshing difficulty in crack propagation simulations, Moës *et al.* (1999) developed an extended FEM (XFEM) by introducing enrichment shape function and level sets method. It allows a crack penetrates elements without remeshing during whole computation process, and this advantage has attracted many researchers.

Besides the problems brought by mesh, another inherent defect also exists in the conventional FEM. At present, most elements are displacement-based in which the nodal displacements are taken as the degrees of freedom (DOFs). For linear elasticity, the finite element equations are usually derived from the principle of minimum potential energy, and relatively more accurate solutions for displacements can be obtained. However, the stress or the internal force solutions are extracted by the constitutive equations consisted of the derivatives of the displacements, so that their precisions and convergences are lower than those for displacements at least one order (in Mindlin–Reissner plate bending problem, the precisions of the shear forces are lower than those for displacements two order). This is the low precision problem for stress solutions of the FEM. In some occasions, such as the pure bending problem modelled by solid elements, if only low-order elements are used, ideal results will not be obtained although the element shapes are not distorted. Furthermore, for some problems in which the stress distributions varies sharply, how to correctly compute stresses is also a big difficulty. As shown in Figure 2, a square plate, with two opposite edges hard simply-supported (SS2) and the other two edges free, is subjected to a uniformly transverse load  $q$ . Because of symmetry, only one quarter of the plate is modelled by a refine mesh with  $64 \times 64$  displacement-based plate elements ARS-Q12 (Soh *et al.*, 2001). However,



The usual FEM results cannot reflect the zero boundary condition of the shear force

**Figure 2.** Distribution of the shear force  $T_x$  along  $y = 0.5L$  in a square plate with two opposite edges hard simply-supported (SS2) and the other two free (Soh *et al.*, 2001)

compared with the semi-analytical solution given by [Kant and Hinton \(1983\)](#), the resulting distribution of the shear force  $T_x$  along  $y = 0.5L$  is not precise. Especially, the zero boundary condition of the shear force at the free edge cannot be reflected.

However, we have to admit that, no matter what defects existing in the FEMs, its position is still irreplaceable for the time being. It still has great significance to develop high-performance FEM that can overcome the shortcomings and improve the performances of the conventional FEM. Although there is no definition for the high-performance FEM, it should possess following features. First, under a coarse mesh, the high-performance FEM will produce much better results than those obtained by the conventional FEM, especially for the problems with drastic stress variation or stress concentration. Second, though the computation cost for a single high-performance finite element may be higher than that for a single conventional element, it will become much lower when simulating the whole structure because a relatively coarse mesh is needed. Third, the high-performance FEM can still perform well when the conventional elements cannot work, such as the elements in the severely distorted meshes. Fourth, the definition of the nodal DOFs is the same as that given for the conventional elements, so that the high-performance FEM can be compiled in current FEM program system without any obstacle.

During the past 60 years, the research on the high-performance FEM has never stopped. Many new ideas have been successfully developed, such as various hybrid stress ([Pian, 1964](#); [Pian and Sumihara, 1984](#); [Pian and Wu, 2006](#); [Wu et al., 1987](#); [Yeo and Lee, 1997](#); [Sze, 2000](#); [Cen et al., 2010](#)) and multi-variable FEMs ([Tian and Pian, 2011](#)), the incompatible or non-conforming FEMs ([Wilson et al., 1973](#); [Taylor et al., 1976](#)), the enhanced assumed strain (EAS) ([Simo and Rifai, 1990](#)) and the directly assumed strain approaches ([MacNeal, 1982](#)), the stabilization matrix method ([Belytschko and Bachrach, 1986](#)), the reduced integration schemes ([Hughes, 1980](#)), the B-bar function method ([Piltner and Taylor, 1997](#)), the quasi-conforming element method ([Chen and Tang, 1981](#); [Tang et al., 1984](#)), the generalized conforming element method ([Long and Huang, 1988](#)), the refined hybrid element method ([Chen, 1992](#)), the smoothed FEM ([Liu et al., 2007](#); [Liu and Quek, 2013](#); [Zeng and Liu, 2018](#)), the variationally consistent FEM ([Liu et al., 2011](#)), new spline FEM ([Chen et al., 2010a, 2010b, 2011](#); [Li et al., 2011](#)), new natural coordinate FEM ([Long et al., 1999a](#); [Long et al., 1999b, 2010](#); [Long and Cen, 2000](#); [Chen et al., 2004, 2008](#); [Li et al., 2008](#); [Cen et al., 2007, 2008](#)), the FE-meshfree element based on partition of unity ([Rajendran and Zhang, 2007](#); [Rajendran et al., 2010](#); [Xu and Rajendran, 2011, 2013](#)) and so on. All of these innovations improved the FEM more or less, but few can perfectly break the limitation brought by the meshes.

[Cen et al. \(2011a\)](#) proposed a concept of *shape-free* FEM. This idea came from their paper published in *Engineering Computations* ([Fu et al., 2010](#)), in which a new kind of FEM whose performances are not affected by element shapes was presented. The eight-node plane quadrilateral element developed in that paper can keep good precision when it is severely distorted, even when the element shape degenerates into a concave quadrangle or a triangle. Recently, some similar models were also proposed by other researchers for plane problem ([Peng et al., 2014a, 2014b](#); [Wang et al., 2016](#); [Xia et al., 2017](#); [Zhou et al., 2016](#)), but seldom developments for 3D problem can be found.

This paper will give a review on some newest developments of the high-performance FEMs achieved by the authors' group ([Cen et al., 2017](#)), including the hybrid stress-function FEM, the hybrid displacement-function FEM and the improved unsymmetric FEM based on the fundamental analytical solutions, and exhibit their applications in plane, crack propagation, plate bending, 3D and shell problems. Some breakthrough points for inherent difficulties existing in current FEM are specially emphasized.

## 2. The hybrid stress-function elements for plane problem

In the stress-function solution method for plane elasticity, the fundamental variable is the stress function  $\phi$ . Substitution of the relationship between the stress vector  $\boldsymbol{\sigma}$  and the stress function  $\phi$ ,  $\boldsymbol{\sigma} = \tilde{\mathbf{R}}(\phi)$ , into the functional of the element complementary energy yields:

$$\Pi_C^e = \Pi_C^{e*} + V_C^{e*} = \frac{1}{2} \iint_{A^e} \tilde{\mathbf{R}}(\phi)^T \mathbf{C} \tilde{\mathbf{R}}(\phi) t dA - \int_{\Gamma^e} [\mathbf{L} \tilde{\mathbf{R}}(\phi)]^T \bar{\mathbf{u}} t ds, \quad (1)$$

in which the stress function  $\phi$  becomes the fundamental variable;  $\mathbf{C}$  is the elasticity matrix of compliances;  $t$ , the thickness of the element;  $A^e$ , the element area;  $\Gamma^e$ , the boundary of the element;  $\mathbf{L}$ , the direction cosine matrix of the element boundary;  $\bar{\mathbf{u}}$ , the displacement vector of the element boundary, which can be interpolated by the element nodal displacement vector  $\mathbf{q}^e$  (same as that of the conventional isoparametric elements).

Accordingly, when formulating the finite element models, instead of directly assuming stresses, the interpolation formula for stress function  $\phi$  is assumed firstly as follows:

$$\phi = \sum_{i=1}^N \phi_i \beta_i = \boldsymbol{\Phi} \boldsymbol{\beta}, \quad (2)$$

where  $N$  is the number of the fundamental analytical solutions  $\phi_i$  used for stress function  $\phi$  in equation (2);  $\beta_i$  ( $i = 1 \sim N$ ) are  $N$  unknown constants;  $\phi_i$  ( $i = 1 \sim N$ ) are  $N$  fundamental analytical solutions (in Cartesian coordinates) of the Airy stress function  $\phi$ , and satisfy the following compatibility equations:

$$\nabla^2 \nabla^2 \phi_i = 0, \quad (\text{isotropic case}) \quad (3)$$

$$\hat{C}_{11} \frac{\partial^4 \phi_i}{\partial y^4} + \hat{C}_{22} \frac{\partial^4 \phi_i}{\partial x^4} + (2\hat{C}_{12} + \hat{C}_{66}) \frac{\partial^4 \phi_i}{\partial x^2 \partial y^2} - 2\hat{C}_{16} \frac{\partial^4 \phi_i}{\partial x \partial y^3} - 2\hat{C}_{26} \frac{\partial^4 \phi_i}{\partial x^3 \partial y} = 0, \quad (\text{anisotropic case}) \quad (4)$$

where  $\hat{C}_{ij} = \hat{C}_{ji}$  are the reduced elastic compliances, and have been defined by [Zienkiewicz and Taylor \(2000\)](#).

The stress function  $\phi$  has three fundamental analytical solutions for constant stress state and four for each other higher order stress states. For establishing equation (2), one should select these fundamental analytical solutions in turn from the lowest-order to higher-order, and ensure that the resulting stress fields possess completeness in Cartesian coordinates. Obviously, the stress fields derived from equation (2) will be more reasonable because they satisfy all control equations. Following the procedure similar to that of the traditional hybrid stress element method ([Pian, 1964](#)), the element stiffness matrix  $\mathbf{K}^*$  and the equivalent nodal load vector can be obtained ([Zhou, 2014](#)). This is the main procedure for construction of the hybrid stress-function (HSF) elements. Because the assume fields are all expressed in terms of Cartesian coordinates, there is no Jacobian determinant existing in the denominator of the final formulae for evaluating  $\mathbf{K}^*$ , so that the main factor leading to sensitivity problem to mesh distortion ([Lee and Bathe, 1993](#)) vanishes naturally.

### 2.1 Plane hybrid stress-function solid element models

[Cen et al. \(2011b\)](#) developed two 8-node and two 12-node quadrilateral hybrid stress-function (HSF) elements for plane elasticity, in which the two 8-node elements, denoted by

HSF-Q8-15 $\beta$  and HSF-Q8-29 $\beta$ , use 15 and 19 fundamental analytical solutions of the stress function; and the two 12-node elements, denoted by HSF-Q12-23 $\beta$  and HSF-Q12-27 $\beta$ , use 23 and 27 solutions. The stress fields of these four elements possess third-, fourth-, fifth- and sixth-order completeness in Cartesian coordinates, respectively. The element shapes are quite free (see Figure 3). Numerical examples show that, the 8-node and 12-node models can produce the exact solutions for pure bending and linear bending problems, respectively, even the element shape degenerates into triangle and concave quadrangle. For higher order problems, they also exhibit much better accuracy, convergence and efficiency than those of the conventional displacement-based elements with same DOFs. Furthermore, the new HSF

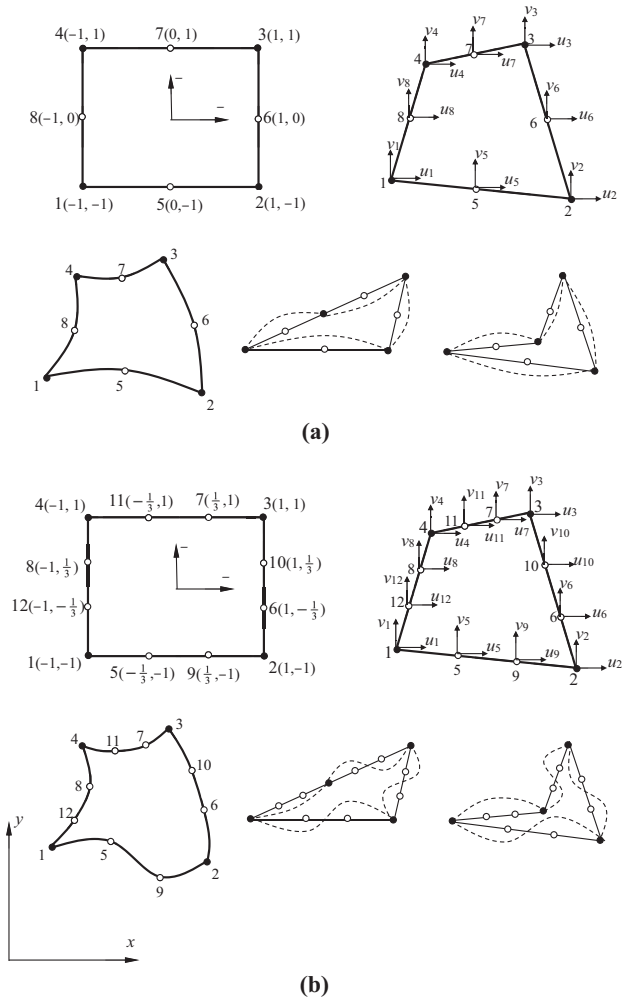


**Figure 3.** Shape-free plane high-order quadrilateral elements (Cen *et al.*, 2011b)

**Notes:** (a) 8-node element with arbitrary shapes; (b) 12-node element with arbitrary shapes

models can avoid volumetric locking naturally. Figure 4 shows a high-order bending problem, a Cook's skew beam under nearly incompressible and plane strain state. The precision of the HSF elements using about only 40 DOFs is almost the same as that obtained by the conventional eight- or nine-node isoparametric elements using about 1,000 DOFs. These HSF elements have also been generalized to the models for anisotropic case (Cen *et al.*, 2011a).

By introducing Allman nodal drilling degrees of freedom (Allman, 1984), Cen *et al.* (2011c) developed a 4-node quadrilateral HSF plane element HSF-Q4 $\theta$ -7 $\beta$  with drilling degrees of freedom by using seven analytical solutions of the stress function. This element exhibits much better and more robust performance than other similar or higher-order displacement-based and hybrid stress elements. It is immune to severe mesh distortion, for example, they can perform well even the element shape degenerates into triangle and concave quadrangle. Zhou and Cen (2015) proposed a shape-free plane quadratic polygonal HSF element HSF-AP-15 $\beta$ . It also exhibits excellent performance for both displacements and stresses.

2.2 The quasi-static crack propagation simulation based on the hybrid stress-function element method with simple remeshing

The HSF element method also benefits solving stress singular problems. Zhou *et al.* (2014) constructed a singular HSF element HSF-Crack for analysis of plane crack tip by using

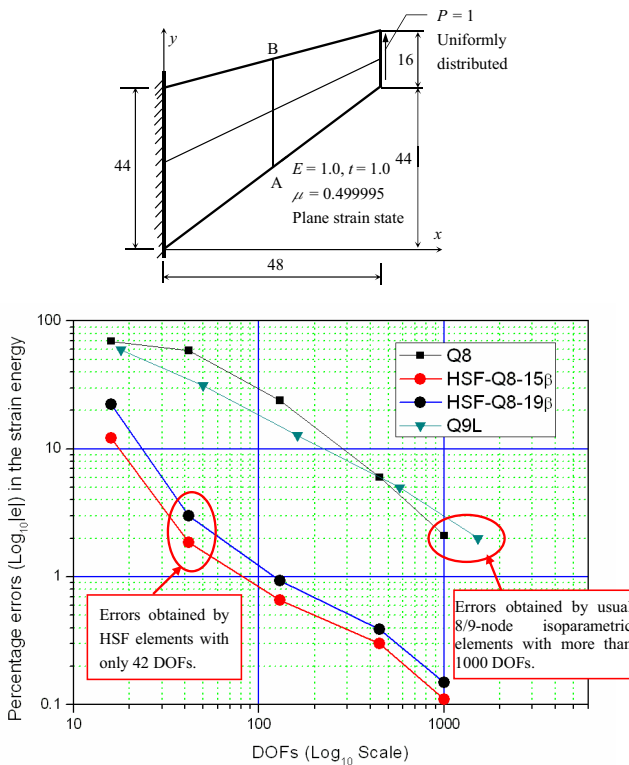


Figure 4. The convergence for the strain energy of Cook's skew beam under plane strain and nearly incompressible state (Cen *et al.*, 2011b)



Williams's analytical solutions for the stress function (Williams, 1957). This element is a shape-free multi-node model with arbitrary polygon. In practical applications, the limitations for its shape, size, number of nodes, number of the trial functions (analytical solutions) are quite small (Figure 5), so that it is very convenient for crack modeling. By combination with the 8-node plane HSF element HSF-Q8-15 $\beta$  (Cen *et al.*, 2011b), the high-precision stress intensity factors can be obtained by using only a few elements, which means the computation costs are quite lower than those of other algorithms. Furthermore, a simple and definite multiple relationship exists between the stress intensity factor and the parameters of the first two solutions of the stress function, so that there is no need for  $J$ -integration or other post-processing procedure.

Then, Zhou *et al.* (2014) proposed a quasi-static crack propagation simulation scheme by applying a simple remeshing strategy with above crack element HSF-Crack and the plane solid element HSF-Q8-15 $\beta$ . This scheme possesses following outstanding features. First, although the configuration of the structure near the crack will become more complicated along with the crack propagation, the shape, the number of nodes, and the size of the crack element at the crack tip can be flexibly adapted for such variation. Second, although the complicated crack propagation path will lead to severe mesh distortion, the computation precision can still be guaranteed because of the merits of the element HSF-Q8-15 $\beta$ . Third, for remeshing in each propagation step, only a relatively coarse mesh is needed, which can be easily achieved by most software products. These features mean that the present scheme is convenient for modeling, and its computation cost is also quite low. Numerical tests demonstrate that the precision and the efficiency of the proposed scheme are better than those of the XFEM (Moës *et al.*, 1999) and smoothed FEM (Nourbakhshnia and Liu, 2011) (see Figure 6). Following the construction procedure of the element HSF-Crack, Cen *et al.* (2016) also proposed a similar scheme by combination of a new low-order crack element HSF-Crack- $\theta$  with drilling degrees of freedom and the element HSF-Q4 $\theta$ -7 $\beta$  (Cen *et al.*, 2011c).

**3. The hybrid displacement-function (HDF) elements for Mindlin–Reissner plate**

How to develop robust finite element models for analysis of Mindlin–Reissner plate is an interesting topic and has attracted many researchers for a long time (Cen and Shang, 2015). An ideal element should be free of shear locking, immune to mesh distortion, and able to

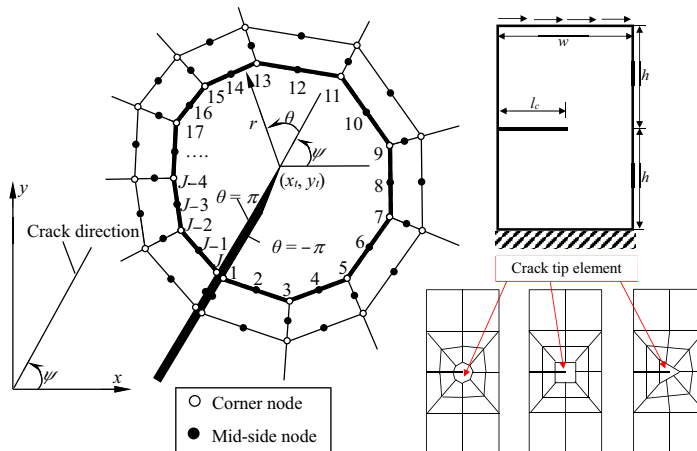


**Figure 5.** Multi-node plane polygonal crack-tip element HSF-Crack and the example meshes for computations (Zhou *et al.*, 2014)



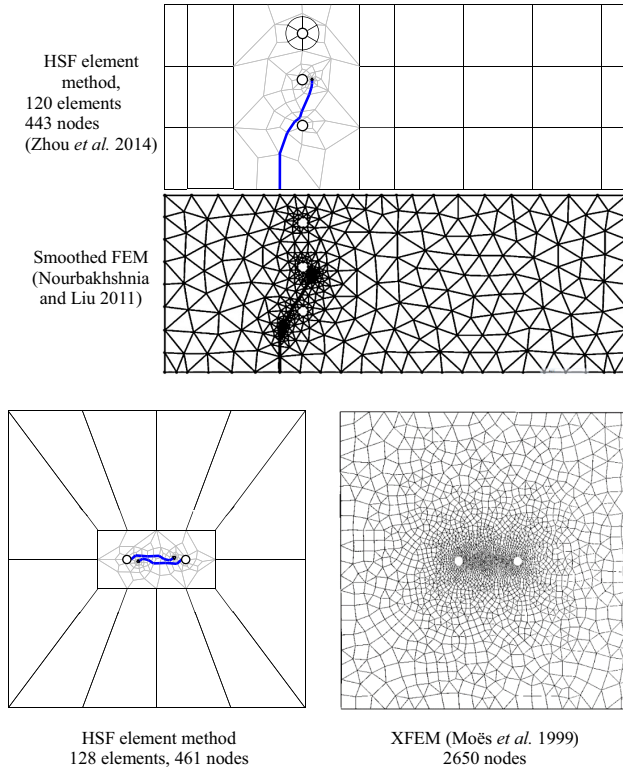


**Figure 6.**  
Comparison of  
different FEMs for  
simulating quasi-  
static crack  
propagation

produce good results for both displacements and internal forces. Although various models have been successfully proposed, few are truly independent of the element shapes. The aforementioned HSF element method provides a new thought for solving this problem. However, the concept of the stress function does not exist in plate problem.

Hu (1984) proved that, in Mindlin–Reissner plate theory, the solutions of deflection  $w$  and rotations  $\psi_x$  and  $\psi_y$  can be expressed by two functions  $F$  and  $f$ :

$$\psi_x = \frac{\partial F}{\partial x} + \frac{\partial f}{\partial y}, \quad \psi_y = \frac{\partial F}{\partial y} - \frac{\partial f}{\partial x}, \quad w = F - \frac{D}{C} \nabla^2 f, \quad (5)$$

in which  $D$  is the bending stiffness of the plate;  $C$ , the shearing stiffness of the plate;  $F$  is active within the whole plate; and  $f$  only appears near the plate edges and reflects edge effects.  $F$  and  $f$  can be defined as displacement functions, and must satisfy following equations:

$$D \nabla^2 \nabla^2 F = q, \quad (6)$$

$$\frac{1}{2} (1 - \mu) D \nabla^2 f - C f = 0, \quad (7)$$

in which  $q$  is the distributed transverse load;  $\mu$  is the Poisson's ratio. The solution of the displacement function  $F$  in equation (6) is the sum of the the general solution  $F^0$  and the particular solution  $F^*$ , in which:

$$D\nabla^2\nabla^2F^0 = 0. \tag{8}$$

Then, according to the geometry and constitutive equations, all components of the stress resultants can be expressed in terms of the displacement function  $F$  and  $f$ :

$$\mathbf{R} = [M_x \quad M_y \quad M_{xy} \quad T_x \quad T_y]^T = \tilde{\mathbf{D}}(F, f), \tag{9}$$

where  $M_x$  and  $M_y$  are bending moments;  $M_{xy}$  is the twisting moment;  $T_x$  and  $T_y$  are the shear forces. These resultant forces satisfy all control equations. Substitution of them into the functional of the element complementary energy yields:

$$\Pi_C^e = \Pi_C^{e*} + V_C^{e*} = \frac{1}{2} \iint_{A^e} \tilde{\mathbf{D}}(F, f)^T \mathbf{C} \tilde{\mathbf{D}}(F, f) dA - \int_{\Gamma^e} [\mathbf{L} \tilde{\mathbf{D}}(F, f)]^T \bar{\mathbf{d}} ds, \tag{10}$$

where  $\mathbf{C}$  is the elastic flexibility matrix for plate;  $\mathbf{L}$  is the direction cosine matrix of the element boundary;  $\bar{\mathbf{d}}$  is the displacements along element edges, which can be interpolated by the element nodal displacement vector  $\mathbf{q}^e$ . (The first-order [Hu, 1984] or the arbitrary order [Jelenic and Papa, 2011] Timoshenko's beam functions are strongly suggested as this interpolation formulae).

When formulating a finite element model, instead of directly assuming resultant force fields, the interpolation formula for displacement functions  $F$  and  $f$  are assumed firstly as follows:

$$\begin{cases} F = F^0 + F^* = \sum_{i=1}^n F_i^0 \beta_i + F^* \\ f = \sum_{j=1}^m f_j \alpha_j \end{cases}, \tag{11}$$

where  $\beta_i$  and  $\alpha_j$  are unknown parameters of the displacement functions;  $F_i^0$  ( $i = 1 \sim n$ ) are first  $n$  analytical solutions (in Cartesian coordinates) of  $F^0$  satisfying equation (8);  $f_j$  ( $j = 1 \sim m$ ) are  $m$  analytical solutions (in Cartesian coordinates) of  $f$  satisfying equation (7);  $F^*$  is the particular solution (in Cartesian coordinates) of  $F$  satisfying equation (6). Other construction procedure is similar to that HSF element method. Finally, according to the principle of the minimum complementary energy, the element stiffness matrix  $\mathbf{K}^*$  and the equivalent nodal load vector can be obtained. This is the main procedure for construction of the HDF elements. Similar to the HSF element method, there is no Jacobian determinant existing in the denominator of the final formulae for evaluating  $\mathbf{K}^*$ , which means that the main factor leading to sensitivity problem to mesh distortion (Lee and Bathe, 1993) is eliminated.

### 3.1 The hybrid displacement-function plate elements insensitive to severe mesh distortion

By only applying the displacement function  $F$ , Cen et al. (2014) presented a four-node, 12-DOF quadrilateral HDF element HDF-P4-11 $\beta$ , in which the first 11 fundamental analytical solutions of  $F^0$  are used so that the corresponding stress resultants fields reach second-order completeness in Cartesian coordinates. This element is quite simple, and exhibits almost the best performance among all existing four-node, 12-DOF quadrilateral

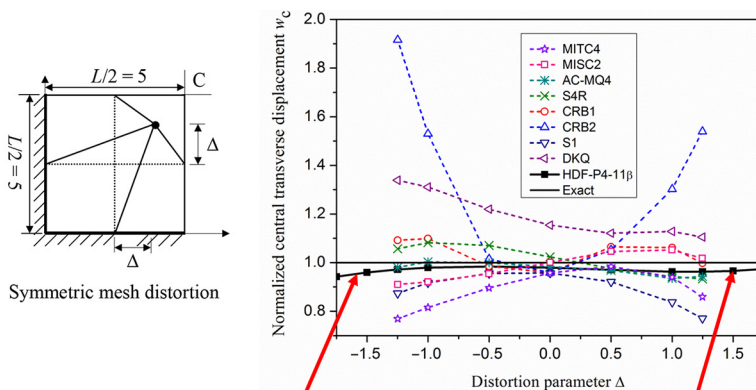
plate bending elements. Especially, it is quite insensitive to severe mesh distortions and can even perform well when element shape is a concave quadrangle or a degenerated triangle.

As shown in Figure 7, a quarter of a thin clamped square plate subjected to uniformly distributed load is considered. This quarter plate is divided by a very coarse mesh ( $2 \times 2$ ), and the central node of the mesh will be moved along the main diagonal of the plate to the two corner nodes.  $\Delta$  is the distortion parameter. It can be seen that, along with the variation of  $\Delta$ , the displacement results obtained by element HDF-P4-11 $\beta$  are quite stable and insensitive to mesh distortion. When an element in the mesh degenerates into a triangle or concave quadrangle (other finite elements cannot work), the model can still keep good precision.

Following above thought, Bao *et al.* (2017) also successfully developed an eight-node, 24-DOF quadrilateral HDF plate element HDF-P8-23 $\beta$  in which the first 23 fundamental analytical solutions of  $F^0$  are applied. It exhibits almost the best performance among all existing eight-node, 24-DOF quadrilateral plate bending elements. Huang *et al.* (2017) also proposed a three-node triangular HDF element HDF-P3-7 $\beta$  for both static and free vibration analyses of Mindlin–Reissner plates. Furthermore, Shang *et al.* (2016) combined the plate element HDF-P4-11 $\beta$  and the plane element HSF-Q4 $\theta$ -7 $\beta$  (with drilling degrees of freedom) to construct a flat shell element HDF-SH4. This new shell element inherits all the advantages from the HDF and HSF element methods. Figure 8 gives the contour plots, calculated by HDF-SH4, of  $y$ -direction displacement of the pinched cylinder with diaphragms ends. It can be seen that, the plots are almost the same no matter regular or distorted mesh is used.

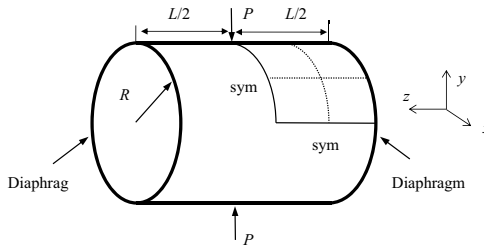
### 3.2 Solving the edge effect difficulty by the hybrid displacement-function element method

As described in Introduction, a kind of special difficulty, i.e. the edge effect phenomenon, is existing in the Mindlin–Reissner plate theory (Arnold and Falk, 1989, 1990). The so-called edge effect, or the boundary layer effect, is the fact that the rotations and stress resultants of a Mindlin–Reissner plate vary sharply in a narrow region at the vicinity of certain types of boundary conditions. Wang *et al.* (2001) pointed out that, accurate predictions of resultants are crucial for the design of a very large floating structure. However, the traditional displacement-based FEM cannot reflect such sharp variation without an extremely refined mesh. Furthermore, the boundary conditions of zero stress resultants cannot be satisfied, either.



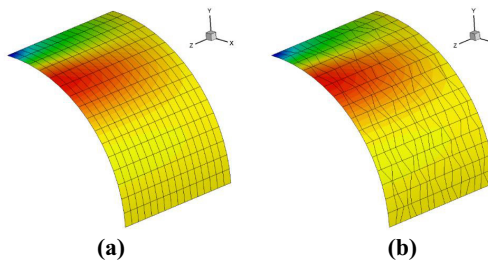
HDF-P4-11 $\beta$  can keep good precision when other elements cannot work (triangle or concave quadrangle)

Figure 7. Sensitivity test for symmetric mesh distortion, clamped plate (Cen *et al.*, 2014)



$$R = 300, L = 600, t = 3, E = 3 \times 10^7, \mu = 0.3, P = 1$$

The pinched cylinder with diaphragms ends



Notes: (a) Regular mesh; (b) distorted mesh

**Figure 8.**  
The contour plots of  
y-direction  
displacement of the  
pinched cylinder on  
different meshes

Shang *et al.* (2015), Shang (2016) firstly gave out two analytical solutions of the displacement function  $f$  satisfying equation (7):

$$F_1 = \frac{1}{D} e^{mx+ny-a_0}, F_2 = \frac{1}{D} (nx - my) e^{mx+ny-a_0}. \quad (12)$$

Then, they used these solutions to extend the HDF elements. After modifying the assumed stress resultants by introducing the exact boundary conditions, two special four-node, 12-DOF quadrilateral HDF plate elements, HDF-P4-Free and HDF-P4-SS1, were successfully formulated for capturing the edges effects along free and soft simply-supported (SS1) boundaries, respectively. When dealing with the edge effect problems, these special elements will be allocated along the corresponding boundary, and the normal HDF element HDF-P4-11 $\beta$  are used in other regions to connect with the special elements.

Figure 9 plots a square plate subjected to a uniformly distributed load  $q$ . Two opposite edges of the plate are hard simply-supported (SS2) and the other two edges free. Owing to symmetry, only a quarter of the plate ABCD is considered. The special element HDF-P4-Free is allocated along the free edge AD, while normal element HDF-P4-11 $\beta$  is used in other region. From Figure 9, it can be seen that, the edge effects of the twisting moment  $M_{xy}$  and the shear force  $T_y$  along AB can be well captured when only a  $4 \times 4$  coarse mesh is used. Especially, the zero boundary condition of the twisting moment  $M_{xy}$  obtained by the current model is exact. However, such good results cannot be obtained by most other higher-order elements, including the 8-node shell element S8R of the Simula/Abaqus, even a refined  $100 \times 100$  mesh is used. To obtain more smoothed results,

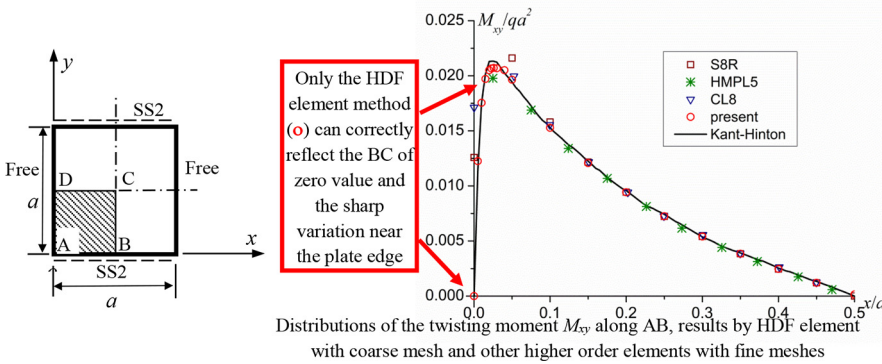
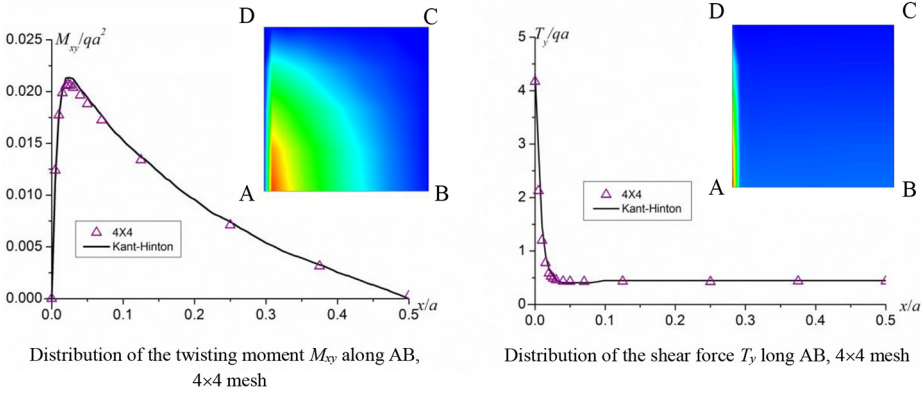


**Figure 9.** The edge effects of a square plate with two opposite edges simply supported and the other two free, span-thickness ratio  $a/h = 50$  (Shang *et al.*, 2015)

Shang *et al.* (2017) proposed an improved HDF (IHDF) element scheme based on a modified complementary energy functional containing Lagrangian multipliers, and developed two new special four-node, 12-DOF IHDF elements, IHDF-P4-Free and IHDF-P4-SS1, for modeling plate behaviors near free and soft simply-supported (SS1) boundaries, respectively. Such new modeling scheme not only greatly improves the precision of the numerical results, but also avoids usage of the additional local coordinate system in original method (Shang *et al.*, 2015).

Following similar procedure, Bao *et al.* (2017) also extended the eight-node, 24-DOF HDF element HDF-P8-23 $\beta$  to two eight-node special HDF elements, HDF-P8-Free and HDF-P8-SS1, for analysis of the edge effects of the free and soft simply-supported boundaries, respectively. Numerical results show they are the best models among the existing eight-node finite elements.

#### 4. An improved unsymmetric finite element method based on the fundamental analytical solutions

The unsymmetric FEM is a kind of Galerkin FEM, in which the test and the trial functions of the displacement fields are different (Rajendran and Liew, 2003; Rajendran *et al.*, 2007; Rajendran, 2010; Liew *et al.*, 2006; Ooi *et al.*, 2004, 2007, 2008). Based on the virtual work principle, the final element stiffness matrix can be written as:

$$\mathbf{K}^e = \iint_{V^e} \bar{\mathbf{B}}^T \hat{\mathbf{D}} \mathbf{B} dV = \int_{-1}^1 \int_{-1}^1 \int_{-1}^1 \frac{\bar{\mathbf{B}}^*}{|\mathbf{J}|} \hat{\mathbf{D}} \hat{\mathbf{B}} |\mathbf{J}| d\xi d\eta d\zeta = \int_{-1}^1 \int_{-1}^1 \bar{\mathbf{B}}^* \hat{\mathbf{D}} \mathbf{B} d\xi d\eta d\zeta \quad (13)$$

where  $\bar{\mathbf{B}} = \bar{\mathbf{B}}^* / |\mathbf{J}|$  is the strain matrix derived from the conventional isoparametric elements;  $\hat{\mathbf{B}}$  is the strain matrix derived from the assumed displacement fields in terms of the Cartesian coordinates;  $|\mathbf{J}|$  is the Jacobi determinant. From equation (13), it can be seen that, although the element stiffness matrix  $\mathbf{K}^e$  is unsymmetric, the Jacobi determinant  $|\mathbf{J}|$  in denominator disappears in the final formula for evaluating  $\mathbf{K}^e$ . Therefore, the main reason that leads to the sensitivity problem to mesh distortion (Lee and Bathe, 1993) does not exist anymore. Several high order models have been developed, including plane 6-node triangular element (Liew *et al.*, 2006), plane 8-node and 9-node quadrilateral elements (Rajendran and Liew, 2003; Rajendran, 2010), 20-node hexahedral element for 3D problem (Ooi *et al.*, 2004), and so on. They are almost immune to severe mesh distortions.

However, because of the limitation for the number of the nodal DOFs, the interpolation formulae for assumed displacement fields in terms of Cartesian coordinates may not be complete. This problem leads to three fetal defects when formulating serendipity (no internal node) plane quadrilateral and 3D hexahedral elements. First, the performance of the low order element cannot be improved. Second, some special shape of the element will lead to interpolation failure so that the element cannot work (for example, the eight-node quadrilateral element degenerate into a triangle) (Ooi *et al.*, 2008). Third, the results for higher-order problems are not consistent when the coordinate axes rotate, i.e. the element exhibits rotational frame dependence (Ooi *et al.*, 2008).

#### 4.1 Improved low-order unsymmetric plane, 3D solid and 3D solid-shell elements that can overcome all defects and break through MacNeal's theorem

In 2012, by applying the fundamental analytical solutions and generalized conforming technique (Long *et al.*, 2009), Cen *et al.* (2012) assumed a new displacement fields that reaches fourth-order completeness in terms of Cartesian coordinates, and constructed a new unsymmetric eight-node, 16-DOF plane quadrilateral element US-ATFQ8. This element can still work well when interpolation failure modes for original unsymmetric element occur (Rajendran and Liew, 2003), and provide the invariance for the coordinate rotation. Furthermore, the exact solutions for constant strain/stress, pure bending and linear bending problems can be obtained by the element US-ATFQ8 using arbitrary severely distorted meshes, and produce more accurate results for other more complicated problems. It should be noted that no other eight-node plane element that can provide exact solutions for linear bending problem is found. Shang *et al.* (2018b) also proposed a successful eight-node unsymmetric element US-Q8 based on self-equilibrium metric stress field for plane orthotropic problem. However, these ideas cannot be directly applied for developing lower-order models.

In 1987, MacNeal (1987) declared his well-known theorem, that is, any four-node, 8-DOF plane membrane element will either lock in in-plane bending or fail to pass a  $C_0$  patch test when the element's shape is an isosceles trapezoid. This conclusion means such low-order elements must be sensitive to mesh distortion, and it almost closes out further effort to extend the linear strain capability of such elements beyond what has already been achieved for rectangular and parallelogram shapes. In 2015, Fotiu (2015) emphasized again that this MacNeal's theorem is hard to be overturned.



In 2015, [Cen et al. \(2015\)](#) and Zhou (2016) proposed a novel unsymmetric FEM by applying fundamental analytical solutions expressed in terms of composite coordinates. For an unsymmetric four-node, 8-DOF plane quadrilateral element, the displacement fields expressed in terms of Cartesian coordinates are rewritten as:

$$\hat{\mathbf{u}} = \begin{Bmatrix} \hat{u} \\ \hat{v} \end{Bmatrix} = \mathbf{P}\boldsymbol{\alpha} = \begin{bmatrix} 1 & 0 & x & 0 & y & 0 & U_7 & U_8 \\ 0 & 1 & 0 & x & 0 & y & V_7 & V_8 \end{bmatrix} \begin{Bmatrix} \alpha_1 \\ \alpha_2 \\ \vdots \\ \alpha_8 \end{Bmatrix}, \quad (14)$$

where  $\alpha_i$  ( $i = 1, 2, \dots, 8$ ) are eight unknown parameters;  $U_7, V_7, U_8, V_8$  are the analytical solutions for pure bending state and expressed in terms of the second form of the quadrilateral area coordinates (QACM-II) ([Chen et al., 2008](#); [Cen et al., 2009](#); [Cen and Zhou, 2016](#)), and they are valid for both isotropic and anisotropic materials. First, because the relationship between the QACM-II and Cartesian coordinate system is always linear, all the features brought by Cartesian coordinates are still kept. Second, as the QACM-II is a kind of local natural coordinates, the rotational frame dependence will not exist even though the trial functions are not completed.

The resulting element, denoted by US-ATFQ4, will never produce interpolation failure, and can exactly pass constant strain/stress patch test no matter its shape is a arbitrarily convex or concave quadrangle, or a degenerated triangle. For the pure bending test given by [Figure 10](#), the computation results are given in [Table I](#). It can be seen that element US-ATFQ4 is the only four-node, 8-DOF model that can provide the exact answers for both pure bending test and the constant strain/stress patch test. Furthermore, there is no rotational frame dependence existing in this element. Thus, the MacNeal's theorem is perfectly broken through. Furthermore, unsymmetric three-node triangular and four-node quadrilateral membrane elements with drilling DOFs that can exhibit excellent performances were also proposed by [Shang et al. \(2018a\)](#), [Shang and Ouyang \(2018\)](#), respectively.

MacNeal's theorem can also be generated to 3D eight-node hexahedral elements and shell elements ([MacNeal, 1992](#)). Actually, how to find a solution strategy for 3D problem is more difficult. [Zhou \(2016\)](#) and [Zhou et al. \(2017\)](#) derived out the fundamental analytical solutions in terms of 3D skew coordinate system ([Yuan et al., 1994](#)) (a kind of local coordinates, also

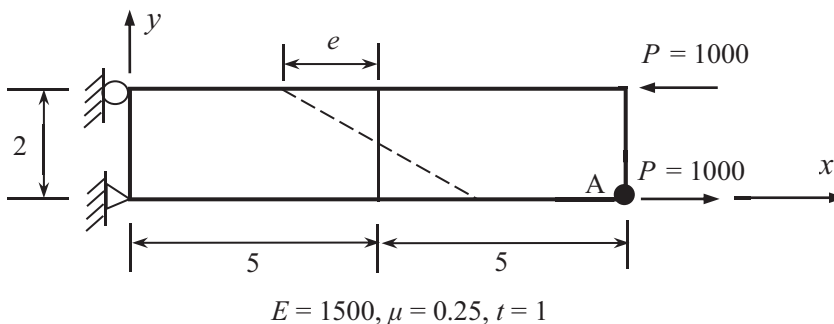


**Figure 10.**  
Pure bending test  
with two distorted  
elements  
([Cen et al., 2015](#))



**Table I.**

Results of the tip deflection  $v_A$  of a pure bending cantilever beam with a distorted parameter  $e$  (Figure 10)

Element models	$e$						
	0	0.5	1	2	3	4	4.9
<i>Elements that cannot pass the <math>C_0</math> patch test</i>							
Q6 (Wilson <i>et al.</i> , 1973)	100	93.21	86.89	92.67	102.42	110.52	116.6
AGQ6-I (Chen <i>et al.</i> , 2004)	100	100	100	100	100	100	100
AGQ6-II (Chen <i>et al.</i> , 2004)	100	100	100	100	100	100	100
QACII6 (Chen <i>et al.</i> , 2008)	100	100	100	100	100	100	100
QAC-ATF4 (Cen <i>et al.</i> , 2009)	100	100	100	100	100	100	100
QACIII6 (Long <i>et al.</i> , 2010)	100	100	100	100	100	100	100
<i>Elements that can pass the <math>C_0</math> patch test</i>							
Q4	28.0	21.0	14.1	9.7	8.3	7.2	6.2
QM6 (Taylor <i>et al.</i> , 1976)	100	80.9	62.7	54.4	53.6	51.2	46.8
P-S (Pian and Sumihara, 1984)	100	81.0	62.9	55.0	54.7	53.1	49.8
SPS (Sze, 2000)	–	–	110.0	120.5	132.7	147.1	162.6
SYHP (Sze, 2000)	–	–	110.0	120.5	132.8	147.5	163.3
CPS4I (Abaqus, 2009)	100	73.53	56.16	50.31	50.38	49.39	46.58
QE2 (Piltner and Taylor, 1995)	100	81.2	63.4	56.5	57.5	57.9	56.9
B-QE4 (Piltner and Taylor, 1997)	100	81.2	63.4	56.5	57.5	57.9	56.9
QACM4 (Cen <i>et al.</i> , 2007)	100	83.8	66.5	60.1	61.4	60.3	56.0
CQAC6 (Long <i>et al.</i> , 2010)	100	83.8	66.5	60.1	61.4	60.3	56.0
F-M QUAD4-P (Rajendran and Zhang, 2007)	9.85	9.94	10.22	11.08	12.00	12.64	12.88
F-M QUAD4-R (Xu and Rajendran, 2011)	99.28	99.28	99.28	99.28	99.28	99.29	99.29
HSF-Q4 $\theta$ -7 $\beta$ (Cen <i>et al.</i> , 2011c)	100	99.93	99.47	95.95	87.14	71.87	52.47
US-ATFQ4	100	100	100	100	100	100	100
Exact	100	100	100	100	100	100	100

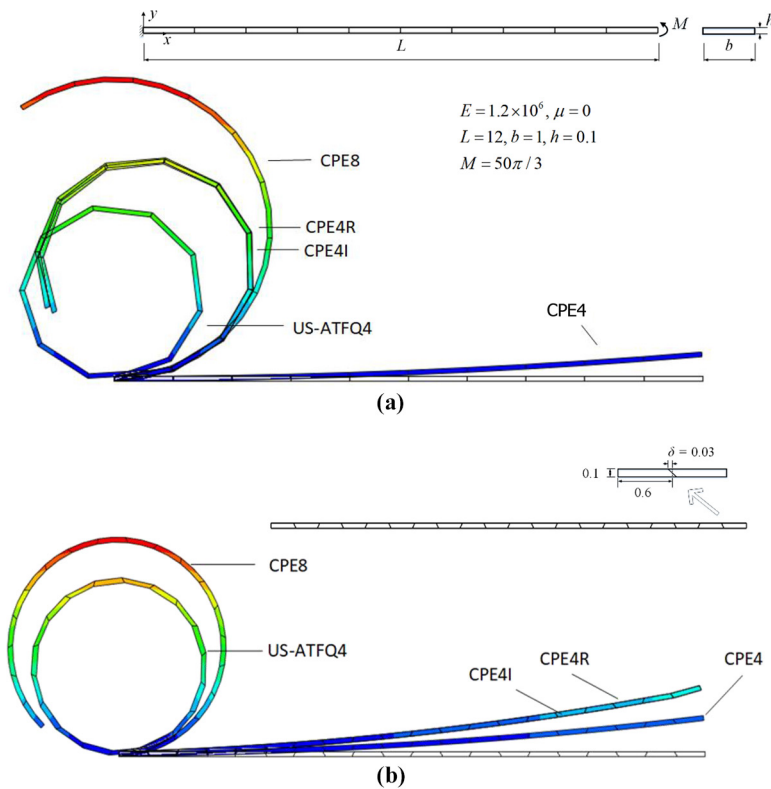
has linear relationship with Cartesian coordinate system) for 3D elasticity (both isotropic and anisotropic materials). Then, they selected the terms corresponding to the pure bending state to assume the displacement fields. Similar to the plane element US-ATFQ4, the resulting 3D unsymmetric eight-node, 24-DOF hexahedral element US-ATFH8 also exhibit super ability for resisting mesh distortion, and can break through the limitations defined by MacNeal's theorem. Recently, by introducing proper shell assumption and assumed natural strain modification for transverse strains, Huang *et al.* (2018) modified the isoparametric displacement fields of element US-ATFH8, and successfully generalized the 3D unsymmetric element US-ATFH8 to a new 3D solid-shell element US-ATFHS8. The new element is able to give highly accurate predictions for shells with different geometric features and loading conditions and is quite insensitive to mesh distortions. In particular, the excellent performance of US-ATFH8 under membrane load is well inherited, which is an outstanding advantage over other shell elements.

#### 4.2 Geometric nonlinear formulations of the improved unsymmetric FEM

Because the improved unsymmetric FEM adopts the fundamental analytical solutions for linear elasticity, some researchers (Cowan and Coombs, 2014) claimed they cannot be applied in nonlinear problems. In fact, the analytical trial functions are only the functions of physical coordinates with material constants. These coordinates and material constants can be updated referring to the current configuration at each iterative step so that it is possible to use them as part of the incremental equations of the updated Lagrangian (UL) formulation.

Recently, Li *et al.* (2018) successfully extended the unsymmetric four-node, 8-DOF element US-ATFQ4 to geometric nonlinear applications. First, the analytical trial functions are updated at each iterative step in the framework of the UL formulation that takes the current configuration, i.e. the configurations at the beginning of an incremental step, as the reference configuration during that step. Then, the Cauchy stresses are updated by the Hughes–Winget method (Hughes and Winget, 1980) to estimate the current stress field. Other procedure is similar to the conventional UL formulations. Numerical examples show that element US-ATFQ4 also possesses amazing performance for geometric nonlinear analysis, no matter whether regular or distorted meshes are used.

Figure 11 shows different deformed shapes of a slender cantilever subjected to a resultant moment at its free end. These shapes are computed by element US-ATFQ4 and other 4-node and 8-node plane quadrilateral elements in CAE platform Simula/Abaqus (Abaqus, 2009), and Figure 11a plots the results by using  $1 \times 10$  regular mesh, while Figure 11b plots the results by using  $1 \times 20$  distorted mesh (isosceles trapezoid). Theoretical analysis shows that the cantilever beam should bend to be a circle. It can be seen that only the unsymmetric four-node, 8-DOF element US-ATFQ4 gives the correct answer, even much better than that obtained by eight-node, 16-DOF element.



**Notes:** (a) Deformations obtained by regular mesh; (b) deformations obtained by distorted mesh

**Figure 11.**  
The final configurations of slender cantilever beam subjected to end resultant moment (Li *et al.*, 2018)

---

Similar situation for geometric nonlinear problems can also be obtained by the 3D unsymmetric eight-node, 24-DOF hexahedral element US-ATFH8 (Zhou *et al.*, 2017). Related results will be reported in near future.

### 5. Concluding remarks

By introducing the fundamental analytical solutions of elasticity, the HSF, the HDF and the improved unsymmetric FEMs are established. They are all the newest developments in the field of high-performance FEM and exhibit advantages from both analytical and numerical approaches. All the successful models exhibit outstanding capacity for resisting various severe mesh distortions, and even perform well when other models cannot work. Some difficulties in the history of the FEM are also broken through, such as the limitations defined by MacNeal's theorem and the edge effect problems of Mindlin–Reissner plate. These efforts promote the progress of the FEM.

The HSF element method is quite simple. It has exhibited its advantages when constructing shape-free high-order plane elements and singular crack tip elements. However, for low-order four-node, 8-DOF element model, the HSF element method has no any merit when compared with the conventional isoparametric element. Furthermore, this method needs an exact displacement mode (not only exact conforming) along element boundary, so that the results will become worse once any edge of plane element is curved, and no proper 3D model can be found.

The improved unsymmetric FEM may be a more promising FEM. Excellent models with high distortion tolerance for plane and 3D elasticity have been successfully developed. But the efficiency of the unsymmetric element stiffness matrix may arouse some doubt from those researchers who have been applying symmetric matrix system for a long time. Actually, by rational design, the unsymmetric matrix will not bring more additional computation costs. In simulations for practical engineering, material nonlinearity and coupled problems often lead to unsymmetric stiffness matrices. All premium CAE products must consider how to solve related problems efficiently (Abaqus, 2009). Furthermore, the precision obtained by several improved unsymmetric elements may reach the precision obtained by several hundreds of isoparametric (symmetric) elements. Therefore, the model composed of the improved unsymmetric elements may have better efficiency. Of course, it cannot say that the improved unsymmetric FEM is completely successful at present, because many problems have not been solved yet. How to extend this method to material nonlinear, contact, dynamic, coupled problems are all interesting topics.

To-date, there is no any other numerical method that can completely replace the FEM. Therefore, it still has great significance and application value to develop high-performance FEMs.

### References

- Abaqus (2009), *HTML Documentation, Abaqus 6.9*, Dassault Systèmes Simulia Corporation, Providence, RI.
- Allman, D.J. (1984), "A compatible triangular element including vertex rotations for plane elasticity analysis", *Computers and Structures*, Vol. 19 Nos 1/2, pp. 1-8.
- Arnold, D.N. and Falk, R.S. (1989), "Edge effects in the reissner-mindlin plate theory", *Analytical and Computational Models for Shells*, pp. 71-90.
- Arnold, D.N. and Falk, R.S. (1990), "The boundary layer for the reissner-mindlin plate model", *SIAM Journal on Mathematical Analysis*, Vol. 21 No. 2, pp. 281-312.

- 
- Bao, Y., Cen, S. and Li, C.F. (2017), "Distortion-resistant and locking-free eight-node elements effectively capturing the edge effects of Mindlin–Reissner plates", *Engineering Computations*, Vol. 34 No. 2, pp. 548-586.
- Bathe, K.J. (1996), *Finite Element Procedures*, Prentice Hall, NJ.
- Belytschko, T. and Bachrach, W.E. (1986), "Efficient implementation of quadrilaterals with high coarse-mesh accuracy", *Computer Methods in Applied Mechanics and Engineering*, Vol. 54 No. 3, pp. 279-301.
- Belytschko, T., Lu, Y.Y. and Gu, L. (1994), "Element free Galerkin method", *International Journal for Numerical Methods in Engineering*, Vol. 37 No. 2, pp. 229-256.
- Cen, S., Chen, X.M. and Fu, X.R. (2007), "Quadrilateral membrane element family formulated by the quadrilateral area coordinate method", *Computer Methods in Applied Mechanics and Engineering*, Vol. 196 Nos 41/44, pp. 4337-4353.
- Cen, S., Chen, X.M., Li, H.G., Du, Y., Fu, X., R. and Guan, N.X. (2008), "Advances in new natural coordinate methods for finite element method", *Engineering Mechanics*, (in Chinese), Vol. 25 No. Sup. I, pp. 18-32.
- Cen, S., Chen, X.M., Li, C.F. and Fu, X.R. (2009), "Quadrilateral membrane elements with analytical element stiffness matrices formulated by the new quadrilateral area coordinate method (QACM-II)", *International Journal for Numerical Methods in Engineering*, Vol. 77 No. 8, pp. 1172-1200.
- Cen, S., Zhang, T., Li, C.F., Fu, X.R. and Long, Y.Q. (2010), "A hybrid-stress element based on Hamilton principle", *Acta Mechanica Sinica*, Vol. 26 No. 4, pp. 625-634.
- Cen, S., Fu, X.R. and Zhou, M.J. (2011a), "8- and 12-node plane hybrid stress-function elements immune to severely distorted mesh containing elements with concave shapes", *Computer Methods in Applied Mechanics and Engineering*, Vol. 200 Nos 29/32, pp. 2321-2336.
- Cen, S., Zhou, M.J. and Fu, X.R. (2011b), "A 4-node hybrid stress-function (HS-F) plane element with drilling degrees of freedom less sensitive to severe mesh distortions", *Computers and Structures*, Vol. 89 Nos 5/6, pp. 517-528.
- Cen, S., Fu, X.R., Zhou, G.H., Zhou, M.J. and Li, C.F. (2011c), "Shape-free finite element method: the plane hybrid Stress-Function (HS-F) element method for anisotropic materials", *Science China Physics, Mechanics and Astronomy*, Vol. 54 No. 4, pp. 653-665.
- Cen, S., Zhou, G.H. and Fu, X.R. (2012), "A shape-free 8-node plane element unsymmetric analytical trial function method", *International Journal for Numerical Methods in Engineering*, Vol. 91 No. 2, pp. 158-185.
- Cen, S., Shang, Y., Li, C.F. and Li, H.G. (2014), "Hybrid displacement function element method: a simple hybrid-Trefftz stress element method for analysis of Mindlin–Reissner plate", *International Journal for Numerical Methods in Engineering*, Vol. 98 No. 3, pp. 203-234.
- Cen, S. and Shang, Y. (2015), "Developments of Mindlin–Reissner plate elements", *Mathematical Problems in Engineering*, Vol. 2015, ID 456740.
- Cen, S., Zhou, P.L., Li, C.F. and Wu, C.J. (2015), "An unsymmetric 4-node, 8-DOF plane membrane element perfectly breaking through MacNeal's theorem", *International Journal for Numerical Methods in Engineering*, Vol. 103 No. 7, pp. 469-500.
- Cen, S. and Zhou, P.L. (2016), "The analytical solutions in terms of the quadrilateral area coordinates for pure bending state and the finite element model breaking MacNeal's theorem", *Chinese Journal of Computational Mechanics*, (in Chinese), Vol. 33 No. 4, pp. 462-468.
- Cen, S., Bao, Y. and Li, C.F. (2016), "Quasi-static crack propagation modeling using shape-free hybrid stress-function elements with drilling degrees of freedom", *International Journal of Computational Methods*, Vol. 13 No. 3, ID 1650014.
- Cen, S., Shang, Y., Zhou, P.L., Zhou, M.J., Bao, Y., Huang, J.B., Wu, C.J. and Li, Z. (2017), "Advances in shape-free finite element methods: a review", *Engineering Mechanics*, (in Chinese), Vol. 34 No. 3, pp. 1-14.

- Chen, W.J. and Tang, L.M. (1981), "Isoparametric quasi-conforming element", *Journal of Dalian Institute of Technology*, (in Chinese), Vol. 20 No. 1, pp. 63-74.
- Chen, W.J. (1992), "Refined hybrid element method and refined quadrilateral plane element", *Journal of Dalian University of Technology*, (in Chinese), Vol. 32 No. 5, pp. 510-519.
- Chen, X.M., Cen, S., Long, Y.Q. and Yao, Z.H. (2004), "Membrane elements insensitive to distortion using the quadrilateral area coordinate method", *Computers and Structures*, Vol. 82 No. 1, pp. 35-54.
- Chen, X.M., Cen, S., Fu, X.R. and Long, Y.Q. (2008), "A new quadrilateral area coordinate method (QACM-II) for developing quadrilateral finite element models", *International Journal for Numerical Methods in Engineering*, Vol. 73 No. 13, pp. 1911-1941.
- Chen, J., Li, C.J. and Chen, W.J. (2010a), "A 17-node quadrilateral spline finite element using the triangular area coordinates", *Applied Mathematics and Mechanics*, Vol. 31 No. 1, pp. 125-134.
- Chen, J., Li, C.J. and Chen, W.J. (2010b), "A family of spline finite elements", *Computers and Structures*, Vol. 88 Nos 11/12, pp. 718-727.
- Chen, J., Li, C.J. and Chen, W.J. (2011), "A 3D pyramid spline element", *Acta Mechanica Sinica*, Vol. 27 No. 6, pp. 986-993.
- Cheng, G.D. and Zhang, H.W. (2007), "Special research reports on the development of the solid mechanics discipline, no. 8: Computational mechanics", *Report on the Development of Solid Mechanics Discipline*, Science and technology of China press, Beijing, (in Chinese).
- Cowan, T. and Coombs, W.M. (2014), "Rotationally invariant distortion resistant finite-elements", *Computer Methods in Applied Mechanics and Engineering*, Vol. 275, pp. 189-203.
- Feng, K. and Shi, Z.C. (2006), *Mathematical Theory of Elastic Structures (Second Printed)*, Science Press, Beijing.
- Fotiu, P.A. (2015), "On shape sensitivity and patch test requirements of incompatible quadrilateral elements in physical coordinates", *Acta Mechanica*, Vol. 226 No. 1, pp. 55-62.
- Fu, X.R., Cen, S., Li, C.F. and Chen, X.M. (2010), "Analytical trial function method for development of new 8-node plane element based on the variational principle containing airy stress function", *Engineering Computations*, Vol. 27 No. 4, pp. 442-463.
- Hu, H.C. (1984), *Variational Principle of Theory of Elasticity with Applications*, Science press, Gordon and Breach; Science publisher, Beijing.
- Huang, J.B., Cen, S., Shang, Y. and Li, C.F. (2017), "A simple triangular hybrid displacement function element for static and free vibration analyses of Mindlin-Reissner plate", *Latin American Journal of Solids and Structures*, Vol. 14 No. 5, pp. 765-804.
- Huang, J.B., Cen, S., Li, Z. and Li, C.F. (2018), "An unsymmetric 8-node hexahedral solid-shell element with high distortion tolerance: Linear formulations", *International Journal for Numerical Methods in Engineering*, Vol. 116 Nos 12/13, pp. 759-783.
- Hughes, T.J.R. (1980), "Generalization of selective integration procedures to anisotropic and nonlinear media", *International Journal for Numerical Methods in Engineering*, Vol. 15 No. 9, pp. 1413-1418.
- Hughes, T.J.R. and Winget, J. (1980), "Finite rotation effects in numerical integration of rate constitutive equations arising in large-deformation analysis", *International Journal for Numerical Methods in Engineering*, Vol. 15 No. 12, pp. 1862-1867.
- Hughes, T.J.R., Cottrell, J.A. and Bazilevs, Y. (2005), "Isogeometric analysis: CAD, finite elements, NURBS, exact geometry and mesh refinement", *Computer Methods in Applied Mechanics and Engineering*, Vol. 194 Nos 39/41, pp. 4135-4195.
- Jelenic, G. and Papa, E. (2011), "Exact solution of 3D Timoshenko beam problem using linked interpolation of arbitrary order", *Archive of Applied Mechanics*, Vol. 81 No. 2, pp. 171-183.
- Kant, T. and Hinton, E. (1983), "Mindlin plate analysis by segmentation method", *Journal of Engineering Mechanics-ASCE*, Vol. 109 No. 2, pp. 537-556.

- Lee, N.S. and Bathe, K.J. (1993), "Effects of element distortion on the performance of isoparametric elements", *International Journal for Numerical Methods in Engineering*, Vol. 36 No. 20, pp. 3553-3576.
- Li, H.G., Cen, S. and Cen, Z.Z. (2008), "Hexahedral volume coordinate method (HVCM) and improvements on 3D Wilson hexahedral element", *Computer Methods in Applied Mechanics and Engineering*, Vol. 197 Nos 51/52, pp. 4531-4548.
- Li, C.J., Chen, J. and Chen, W.J. (2011), "A 3D hexahedral spline element", *Computers and Structures*, Vol. 89 Nos 23/24, pp. 2303-2308.
- Li, Z., Cen, S., Wu, C.J., Shang, Y. and Li, C.F. (2018), "High-performance geometric nonlinear analysis with the unsymmetric 4-node, 8-DOF plane element US-ATFQ4", *International Journal for Numerical Methods in Engineering*, Vol. 114 No. 9, pp. 931-954.
- Liew, K.M., Rajendran, S. and Wang, J. (2006), "A quadratic plane triangular element immune to quadratic mesh distortions under quadratic displacement fields", *Computer Methods in Applied Mechanics and Engineering*, Vol. 195 Nos 9/12, pp. 1207-1223.
- Liu, G.R., Dai, K.Y. and Nguyen, T.T. (2007), "A smoothed finite element method for mechanics problems", *Computational Mechanics*, Vol. 39 No. 6, pp. 859-877.
- Liu, G.R., Nguyen-Xuan, H. and Nguyen-Thoi, T. (2011), "A variationally consistent  $\alpha$ FEM (VC $\alpha$ FEM) for solution bounds and nearly exact solution to solid mechanics problems using quadrilateral elements", *International Journal for Numerical Methods in Engineering*, Vol. 85 No. 4, pp. 461-497.
- Liu, G.R. and Quek, S.S. (2013), *The Finite Element Method: A Practical Course*, 2nd ed., Butterworth-Heinemann, Oxford.
- Long, Y.Q. and Huang, M.F. (1988), "A generalized conforming isoparametric element", *Applied Mathematics and Mechanics*, Vol. 9 No. 10, pp. 929-936.
- Long, Z.F. and Cen, S. (2000), *Generalized Conforming Element Theory and Quadrilateral Area Coordinate Method*, China University of Mining and Technology Press, Xuzhou, (in Chinese).
- Long, Z.F. and Cen, S. (2001), *New Monograph of Finite Element Method: principle.programming. developments*, China Hydraulic and Water-power Press, Beijing, (in Chinese).
- Long, Y.Q., Cen, S. and Long, Z.F. (2009), *Advanced Finite Element Method in Structural Engineering*, Springer, Heidelberg and Tsinghua University Press, Beijing.
- Long, Y.Q., Li, J.X., Long, Z.F. and Cen, S. (1999a), "Area coordinates used in quadrilateral elements", *Communications in Numerical Methods in Engineering*, Vol. 15 No. 8, pp. 533-545.
- Long, Z.F., Li, J.X., Cen, S. and Long, Y.Q. (1999b), "Some basic formulae for area coordinates used in quadrilateral elements", *Communications in Numerical Methods in Engineering*, Vol. 15 No. 12, pp. 841-852.
- Long, Z.F., Cen, S., Wang, L., Fu, X.R. and Long, Y.Q. (2010), "The third form of the quadrilateral area coordinate method (QACM-III): theory, application, and scheme of composite coordinate interpolation", *Finite Elements in Analysis and Design*, Vol. 46 No. 10, pp. 805-818.
- Lu, X.Z., Liu, K.Q., Cen, S., Xu, Z. and Lin, L. (2015), "Comparing different fidelity models for the impact analysis of large commercial aircrafts on a containment building", *Engineering Failure Analysis*, Vol. 57, pp. 254-269.
- Lu, X.Z., Tian, Y., Cen, S., Guan, H., Xie, L.L. and Wang, L.S. (2018), "A high-performance quadrilateral flat shell element for seismic collapse simulation of tall buildings and its implementation in OpenSees", *Journal of Earthquake Engineering*, Vol. 22 No. 9, pp. 1662-1682.
- MacNeal, R.H. (1982), "Derivation of element stiffness matrices by assumed strain distributions", *Nuclear Engineering Design*, Vol. 70 No. 1, pp. 3-12.
- MacNeal, R.H. (1987), "A theorem regarding the locking of tapered four-node membrane elements", *International Journal for Numerical Methods in Engineering*, Vol. 24 No. 9, pp. 1793-1799.



- MacNeal, R.H. (1992), "On the limits of element perfectability", *International Journal for Numerical Methods in Engineering*, Vol. 35 No. 8, pp. 1589-1601.
- Moës, N., Dolbow, J. and Belytschko, T. (1999), "A finite element method for crack growth without remeshing", *International Journal for Numerical Methods in Engineering*, Vol. 46 No. 1, pp. 131-150.
- Nourbakhshnia, N. and Liu, G.R. (2011), "A quasi-static crack growth simulation based on the singular ES-FEM", *International Journal for Numerical Methods in Engineering*, Vol. 88 No. 5, pp. 473-492.
- Ooi, E.T., Rajendran, S. and Yeo, J.H. (2004), "A 20-node hexahedral element with enhanced distortion tolerance", *International Journal for Numerical Methods in Engineering*, Vol. 60 No. 15, pp. 2501-2530.
- Ooi, E.T., Rajendran, S. and Yeo, J.H. (2007), "Extension of unsymmetric finite elements US-QUAD8 and US-HEXA20 for geometric nonlinear analyses", *Engineering Computations*, Vol. 24 No. 4, pp. 407-431.
- Ooi, E.T., Rajendran, S. and Yeo, J.H. (2008), "Remedies to rotational frame dependence and interpolation failure of US-QUAD8 element", *Communications in Numerical Methods in Engineering*, Vol. 24 No. 11, pp. 1203-1217.
- Peng, Y.J., Zhang, L.J., Pu, J.W. and Guo, Q. (2014a), "A two-dimensional base force element method using concave polygonal mesh", *Engineering Analysis with Boundary Elements*, Vol. 42, pp. 45-50.
- Peng, Y.J., Zong, N.N., Zhang, L.J. and Pu, J.W. (2014b), "Application of 2D base force element method with complementary energy principle for arbitrary meshes", *Engineering Computations*, Vol. 31 No. 4, pp. 691-708.
- Pian, T.H.H. (1964), "Derivation of element stiffness matrices by assumed stress distributions", *AIAA Journal*, Vol. 2 No. 7, pp. 1333-1336.
- Pian, T.H.H. and Wu, C.C. (2006), *Hybrid and Incompatible Finite Element Methods*, Chapman & Hall/CRC, Boca Raton.
- Pian, T.H.H. and Sumihara, K. (1984), "Rational approach for assumed stress finite elements", *International Journal for Numerical Methods in Engineering*, Vol. 20 No. 9, pp. 1685-1695.
- Piltner, R. and Taylor, L. (1995), "A quadrilateral mixed finite element with two enhanced strain modes", *International Journal for Numerical Methods in Engineering*, Vol. 38 No. 11, pp. 1783-1808.
- Piltner, R. and Taylor, R.L. (1997), "A systematic constructions of B-bar functions for linear and nonlinear mixed-enhanced finite elements for plane elasticity problems", *International Journal for Numerical Methods in Engineering*, Vol. 44 No. 5, pp. 615-639.
- Rajendran, S. (2010), "A technique to develop mesh-distortion immune finite elements", *Computer Methods in Applied Mechanics and Engineering*, Vol. 199 Nos 17/20, pp. 1044-1063.
- Rajendran, S. and Liew, K.M. (2003), "A novel unsymmetric 8-node plane element immune to mesh distortion under a quadratic displacement field", *International Journal for Numerical Methods in Engineering*, Vol. 58 No. 11, pp. 1713-1748.
- Rajendran, S. and Zhang, B.R. (2007), "A FE-meshfree QUAD4 element based on partition of Unity", *Computer Methods in Applied Mechanics and Engineering*, Vol. 197 Nos 1/4, pp. 128-147.
- Rajendran, S., Ooi, E.T. and Yeo, J.H. (2007), "Mesh-distortion immunity assessment of QUAD8 elements by strong-form patch tests", *Communications in Numerical Methods in Engineering*, Vol. 23 No. 2, pp. 157-168.
- Rajendran, S., Zhang, B.R. and Liew, K.M. (2010), "A partition of Unity-based 'FE-meshfree' QUAD4 element for geometric non-linear analysis", *International Journal for Numerical Methods in Engineering*, Vol. 82 No. 12, pp. 1574-1680.



- Shang, Y. (2016), "Shape-free plate/shell finite elements based on displacement functions and solution strategies for edge effects", Doctoral Dissertation of Tsinghua University, Beijing, (in Chinese).
- Shang, Y., Cen, S. and Li, C.F. (2016), "A 4-node quadrilateral flat shell element formulated by the shape-free HDF plate and HSF membrane elements", *Engineering Computations*, Vol. 33 No. 3, pp. 713-741.
- Shang, Y., Cen, S., Li, C.F. and Huang, J.B. (2015), "An effective hybrid displacement function element method for solving the edge effect of Mindlin–Reissner plate", *International Journal for Numerical Methods in Engineering*, Vol. 102 No. 8, pp. 1449-1487.
- Shang, Y., Cen, S., Li, Z. and Li, C.F. (2017), "Improved hybrid displacement function (IHDF) element scheme for analysis of Mindlin–Reissner plate with edge effect", *International Journal for Numerical Methods in Engineering*, Vol. 111 No. 12, pp. 1120-1169.
- Shang, Y., Cen, S., Qian, Z.H. and Li, C.F. (2018a), "High-performance unsymmetric 3-node triangular membrane element with drilling DOFs can correctly undertake in-plane moments", *Engineering Computations*, Vol. 35 No. 7, pp. 2543-2556.
- Shang, Y., Cen, S. and Zhou, M.J. (2018b), "8-node unsymmetric distortion-immune element based on airy stress solutions for plane orthotropic problems", *Acta Mechanica*, Vol. 229 No. 12, pp. 5031-5049.
- Shang, Y. and Ouyang, W. (2018), "4-node unsymmetric quadrilateral membrane element with drilling DOFs insensitive to severe mesh-distortion", *International Journal for Numerical Methods in Engineering*, Vol. 113 No. 10, pp. 1589-1606.
- Simo, J.C. and Rifai, M.S. (1990), "A class of mixed assumed strain methods and the method of incompatible modes", *International Journal for Numerical Methods in Engineering*, Vol. 29 No. 8, pp. 1595-1638.
- Soh, A.K., Cen, S., Long, Y.Q. and Long, Z.F. (2001), "A new twelve DOF quadrilateral element for analysis of thick and thin plates", *European Journal of Mechanics A-Solids*, Vol. 20 No. 2, pp. 299-326.
- Sze, K.Y. (2000), "On immunizing five-beta hybrid stress element models from 'trapezoidal locking' in practical analyses", *International Journal for Numerical Methods in Engineering*, Vol. 47 No. 4, pp. 907-920.
- Tang, L.M., Chen, W.J. and Liu, Y.G. (1984), "Formulation of quasi-conforming element and Hu-Washizu principle", *Computers and Structures*, Vol. 19 Nos 1/2, pp. 247-250.
- Taylor, R.L., Beresford, P.J. and Wilson, E.L. (1976), "A non-conforming element for stress analysis", *International Journal for Numerical Methods in Engineering*, Vol. 10 No. 6, pp. 1211-1219.
- Tian, Z.S. and Pian, T.H.H. (2011), *Multivariable Variational Principles and Multivariable Finite Element Methods*, Science Press, Beijing, (in Chinese).
- Turner, M.J., Clough, R.W., Martin, H.C. and Topp, L.J. (1956), "Stiffness and deflection analysis of complex structures", *Journal of the Aeronautical Science*, Vol. 23 No. 9, pp. 805-823.
- Wang, C., Zhang, X. and Hu, P. (2016), "New formulation of quasi-conforming method: a simple membrane element for analysis of planar problems", *European Journal of Mechanics/A Solids*, Vol. 60, pp. 122-133.
- Wang, C.M., Xiang, Y., Utsunomiya, T. and Watanabe, E. (2001), "Evaluation of modal stress resultants in freely vibrating plates", *International Journal of Solids and Structures*, Vol. 38 Nos 36/37, pp. 6525-6558.
- Williams, M.L. (1957), "On the stress distribution at the base of a stationary crack", *Journal of Applied Mechanics*, Vol. 24, pp. 109-114.
- Wilson, E.L., Tayler, R.L., Doherty, W.P. and Ghaboussi, T. (1973), "Incompatible displacement models", *Numerical and Computational Methods in Structural Mechanics*, Academic Press, New York, NY, pp. 43-57.

- Wu, C.C., Huang, M.G. and Pian, T.H.H. (1987), "Consistency condition and convergence criteria of incompatible elements: general formulation of incompatible functions and its application", *Computers and Structures*, Vol. 27 No. 5, pp. 639-644.
- Xia, Y., Zheng, G.J. and Hu, P. (2017), "Incompatible modes with Cartesian coordinates and application in quadrilateral finite element formulation", *Computational and Applied Mathematics*, Vol. 36 No. 2, pp. 859-875.
- Xu, J.P. and Rajendran, S. (2011), "A partition-of-Unity based 'FE-Meshfree' QUAD4 element with radial-polynomial basis functions for static analyses", *Computer Methods in Applied Mechanics and Engineering*, Vol. 200 Nos 47/48, pp. 3309-3323.
- Xu, J.P. and Rajendran, S. (2013), "A 'FE-Meshfree' TRIA3 element based on partition of unity for linear and geometry nonlinear analyses", *Computational Mechanics*, Vol. 51 No. 6, pp. 843-864.
- Yeo, S.T. and Lee, B.C. (1997), "New stress assumption for hybrid stress elements and refined four-node plane and eight-node brick elements", *International Journal for Numerical Methods in Engineering*, Vol. 40 No. 16, pp. 2933-2952.
- Yuan, K.Y., Huang, Y.S., Yang, H.T. and Pian, T.H.H. (1994), "The inverse mapping and distortion measures for 8-node hexahedral isoparametric elements", *Computational Mechanics*, Vol. 14 No. 2, pp. 189-199.
- Zeng, W. and Liu, G.R. (2018), "Smoothed finite element methods (S-FEM): an overview and recent developments", *Archives of Computational Methods in Engineering*, Vol. 25 No. 2, pp. 397-435.
- Zhang, Q. and Cen, S. (2016), *Multiphysics Modeling: numerical Methods and Engineering Applications*, Elsevier and Tsinghua University Press, Beijing.
- Zhou, M.J. (2014), "Shape-Free plane hybrid Stress-Function finite element method", Doctoral Dissertation of Tsinghua University, Beijing, (in Chinese).
- Zhou, P.L. (2016), "Shape-Free low-order unsymmetric finite elements and polygonal hybrid Stress-Function element", Doctoral Dissertation of Tsinghua University, Beijing, (in Chinese).
- Zhou, P.L. and Cen, S. (2015), "A novel shape-free plane quadratic polygonal hybrid stress-function element", *Mathematical Problems in Engineering*, Vol. 2015, ID 491325.
- Zhou, M.J., Cen, S., Bao, Y. and Li, C.F. (2014), "A quasi-static crack propagation simulation based on shape-free hybrid stress-function finite elements with simple remeshing", *Computer Methods in Applied Mechanics and Engineering*, Vol. 275, pp. 159-188.
- Zhou, P.L., Cen, S., Huang, J.B., Li, C.F. and Zhang, Q. (2017), "An unsymmetric 8-node hexahedral element with high distortion tolerance", *International Journal for Numerical Methods in Engineering*, Vol. 109 No. 8, pp. 1130-1158.
- Zhou, X.C., Meng, Z.L. and Luo, Z.X. (2016), "New nonconforming finite elements on arbitrary convex quadrilateral meshes", *Journal of Computational and Applied Mathematics*, Vol. 296, pp. 798-814.
- Zhuang, Z., Zhang, F., Cen, S., You, X.C., Yu, X.G., Mu, Q.C., Xu, M. and Bai, R. (2005), *Abaqus Non-Linear Finite Element Analysis and Examples*, Science Press, Beijing, (in Chinese).
- Zienkiewicz, O.C. and Taylor, R.L. (2000), "The finite element method", Vol. 2. *Solid Mechanics*, 5th ed., Butterworth-Heinemann: Oxford.

**Corresponding author**

Song Cen can be contacted at: [censong@mail.tsinghua.edu.cn](mailto:censong@mail.tsinghua.edu.cn)

---

For instructions on how to order reprints of this article, please visit our website:

[www.emeraldgroupublishing.com/licensing/reprints.htm](http://www.emeraldgroupublishing.com/licensing/reprints.htm)

Or contact us for further details: [permissions@emeraldinsight.com](mailto:permissions@emeraldinsight.com)